Acoustic and geoacoustic inverse problems in randomly perturbed shallow-water environments

Laure Dumaz,[1,a)] Josselin Garnier,[2,b)] and Guilhem Lepoultier[3]
[1]*Ceremade, Université Paris-Dauphine, 75016 Paris, France*
[2]*Centre de Mathématiques Appliquées, Ecole Polytechnique, 91128 Palaiseau Cedex, France*
[3]*Sivienn, 29570 Roscanvel, France*

(Received 23 January 2019; revised 30 May 2019; accepted 25 June 2019; published online 25 July 2019)

The main goal of this paper is to estimate the regional acoustic and geoacoustic shallow-water environment from data collected by a vertical hydrophone array and transmitted by distant time-harmonic point sources. The aim is to estimate the statistical properties of the random fluctuations of the index of refraction in the water column and the characteristics of the sea bottom. It is explained from first principles how acoustic wave propagation can be expressed as Markovian dynamics for the complex mode amplitudes of the sound pressure. This makes it possible to express the cross moments of the sound pressure in terms of the parameters to be estimated. Then it is shown how the estimation problem can be formulated as a nonlinear inverse problem using this formulation, which can be solved by minimization of a misfit function. The method is applied to experimental data collected by the Acoustic Laboratory for Marine Applications system. A Bayesian analysis quantifies the uncertainty of the estimation. https://doi.org/10.1121/1.5116569

[BTH] Pages: 458–469

I. INTRODUCTION

In this paper we consider acoustic wave propagation in a randomly perturbed shallow-water waveguide with an absorbing sea bottom. The random perturbations of the index of refraction are due to internal waves, which induce temperature and salinity fluctuations, and the sea bottom is made of sediments, which induce dissipation. In the regime where random perturbations and dissipation are small and propagation distance large, it is possible to get an effective description of the acoustic wave propagation in terms of Markovian dynamics for the complex mode amplitudes of the expansion of the pressure field to the guided modes of the unperturbed and non-dissipative waveguide. These Markovian dynamics involve coupling terms between guided modes and mode-dependent dispersion and loss terms. The coupling terms between guided modes come from the random perturbations in the water column. The effective dispersion and loss terms come from two effects: the random perturbations in the water column induce coupling between the guided and radiative modes, and the deterministic dissipation in the sediment layer induces an exponential decay of the guided mode amplitudes. Both effects generate an irreversible, mode-dependent loss of energy carried by the guided modes.

The mathematical literature contains a lot of results on wave propagation in randomly perturbed waveguides motivated by underwater acoustics, see, for example, Refs. 1–3. Those results derive from first principles and make it possible to relate the coefficients of the effective Markovian model to the physical parameters of the waveguide (in particular, the statistics of the fluctuations of the index of refraction and the complex acoustic impedance of the sea bottom). The mathematical statements also make it clear in which sense the Markovian model approximates the random dynamics of the mode amplitudes in the waveguide, because there are subtle effects that follow from the fact that the results are established and only hold in a weak topology, as explained in Appendix B. Comparisons between theory and numerical simulations show good agreement, both for direct and synthetic inverse problems,[4] but there has not been, so far, much comparison between the detailed mathematical predictions and real experiments. On the other hand, the physics literature contains many theoretical results essentially based on coupled mode equations.[5–10] However, the equations are derived ad hoc and it is not always straightforward to relate the coefficients of the effective equations to the physical and statistical parameters of the medium. This is problematic as we have in mind to use such results to solve an inverse problem based on real experimental data. Geo-acoustic inversion has, in general, the form of a matched field process.[11] Severe problems appear, however, when modeling shallow-water acoustic propagation at ranges beyond a few kilometers in the frequency band of 1 kHz and higher because of ocean sound speed fluctuations.[12] Here, we deal with a situation where the observed field is incoherent and the information is encoded in the cross-correlation function (or cross power spectral density).

As we will see in this paper, the effective attenuation of the mode amplitudes plays a key role. In the physics literature, modal attenuation coefficients are introduced directly into the coupled mode equations without derivation from first principles.[8,13,14] On the other hand, most mathematical studies do not take into account the attenuation of the bottom layer. Even though dissipation is weak, it still plays an

[a)]Also at: Sivienn, 29570 Roscanvel, France.
[b)]Also at: Sivienn, 29570 Roscanvel, France. Electronic mail: josselin.garnier@polytechnique.edu

important role in long-range propagation. For the direct problem point of view the equipartition regime that is well characterized by Gaussian statistics[15] and a scintillation index (relative intensity variance) that is close to one in the absence of dissipation looks very different in the presence of weak attenuation and it may give rise to high fluctuations in intensity. This was first pointed out by Creamer.[8] For the inverse problem point of view, signals measured by hydrophone array can be processed to extract these attenuation coefficients, which, in turn, make it possible to get information on the medium, in particular, the bottom properties. In Refs. 16 and 17 the seabed attenuation is inferred from measured modal dispersion and/or modal attenuation. In Ref. 18, the measurements of the reverberation vertical coherence are used to estimate acoustic seabed properties (see also Ref. 19 for the use of longitudinal horizontal coherence). Here, we use the full expressions of the modal attenuation coefficients (in terms of the seabed properties and fluctuations of the sound speed in the water column) and of the modal coupling coefficients to solve the inverse problem when the recorded wavefield is incoherent. We exploit data from at-sea experiments based on DGA's Acoustic Laboratory for Marine Applications (ALMA) system.[20] The signals recorded by the hydrophone array can be processed by cross-correlation calculations to estimate the properties of the medium, as we show in Sec. V.

The paper is organized as follows. The direct problem is analyzed in Secs. II–IV. Section III is a review of the modal decomposition of the sound pressure in a homogeneous, non-dissipative waveguide. Section IV describes the Markovian dynamics of the mode amplitudes in a random, dissipative waveguide. The inverse problem is formulated and solved using experimental data in Sec. V.

II. WAVE PROPAGATION IN WAVEGUIDES

Our model consists of a two-dimensional waveguide with the range axis denoted by $x \in \mathbb{R}$ and the transverse coordinate denoted by $z \in [0, +\infty)$. We suppose that the sea depth is constant and equal to z_b. When $z \in [0, z_b]$, the medium is water; when $z > z_b$, it becomes sediments. A point-like source at a fixed position $(x, z) = (0, z_0)$ transmits a time-harmonic signal at frequency ω, which is collected by a vertical array of receivers (hydrophones) at $x = x_a$. We consider that the density ρ is stepwise constant and equal to ρ_w in the water and ρ_s in the sediments. The acoustic pressure $\hat{p}(x, z)$ satisfies the Helmholtz equation,

$$\left[(\partial_x^2 + \partial_z^2) + \frac{\omega^2}{c(x,z)^2}\right]\hat{p}(x,z) = \delta(x)\delta(z - z_0), \tag{1}$$

for $x \in \mathbb{R}$, $z \in (0, z_b) \cup (z_b, +\infty)$, where $c(x, z)$ is the sound speed at position (x, z). The acoustic pressure also satisfies the Dirichlet boundary condition on the top of the water column $\hat{p}(x, 0) = 0$ for all $x \in \mathbb{R}$, and the continuity conditions at depth z_b : $\hat{p}(x, z_b^-) = \hat{p}(x, z_b^+)$ and $\partial_z \hat{p}(x, z_b^-)/\rho_w = \partial_z \hat{p}(x, z_b^+)/\rho_s$.

Remark. *The model (1) can be derived from a more realistic three-dimensional situation, in which the pressure field $\hat{P}$ satisfies in cylindrical coordinates*

$$\left[\partial_r^2 + \frac{1}{r}\partial_r + \frac{1}{r^2}\partial_\theta^2 + \partial_z^2 + \frac{\omega^2}{c(r,z)^2}\right]\hat{P} = \frac{1}{2\pi r}\delta(r)\delta(z - z_0).$$

The solution is radially symmetric and, if we neglect a near field factor of the form $\hat{p}/r^{5/2}$, then the scaled pressure field $\hat{p}(r, z) = \sqrt{r}\hat{P}(r, z)$ satisfies Eq. (1).

Let us now describe the results we obtain in this model. We compute in Sec. III the pressure for an ideal (homogeneous) waveguide. Next we analyze how it behaves when the sound speed in the water is no longer constant, but weakly randomly perturbed and the sediments are weakly dissipative. The wave modes interact with each other, and the asymptotic regime with small perturbation and large propagation distance is studied in Sec. IV. In particular, we compute correlations of the recorded pressure signals for hydrophones located in a vertical segment for exponentially decaying correlations of the medium in Sec. IV E.

III. HOMOGENEOUS WAVEGUIDE

In this section, we consider a wave speed $c(x, z)$ that is constant both in the water and in the sediments,

$$c_0(z) = c_w \mathbf{1}_{[0,z_b]}(z) + c_s \mathbf{1}_{(z_b,+\infty)}(z), \tag{2}$$

with $c_s > c_w$ (Pekeris waveguide). We denote $k_w = \omega/c_w$ and $k_s = \omega/c_s$. There is no dissipation, no fluctuation along the x axis. The analysis of the perfect waveguide is classical;[21] we only give the main results. The Helmholtz operator has a spectrum of the form

$$(-\infty, k_s^2) \cup \{k_{zN}^2, \ldots, k_{z1}^2\}, \tag{3}$$

where the N modal wavenumbers k_{zj} are positive and $k_s^2 < k_{zN}^2 < \cdots < k_{z1}^2 < k_w^2$. The generalized eigenfunctions ϕ_γ associated with the spectral parameter γ in the continuous spectrum $(-\infty, k_s^2)$ and the eigenfunctions ϕ_j, $j = 1, \ldots, N$, associated with the discrete spectrum, are given in Appendix A. Any function can be expanded on the set of the eigenfunctions of the Helmholtz operator. In particular, any solution of the Helmholtz equation in homogeneous medium can be expanded as

$$\hat{p}(x,z) = \sum_{j=1}^{N} \hat{p}_j(x)\phi_j(z) + \int_{-\infty}^{k_s^2} \hat{p}_\gamma(x)\phi_\gamma(z)d\gamma. \tag{4}$$

The modes for $j = 1, \ldots, N$ are guided, the modes for $\gamma \in (0, k_s^2)$ are radiating, and the modes for $\gamma \in (-\infty, 0)$ are evanescent. Indeed, the complex mode amplitudes satisfy $\partial_x^2 \hat{p}_j + k_{zj}^2 \hat{p}_j = 0$ for $j = 1, \ldots, N$ and $\partial_x^2 \hat{p}_\gamma + \gamma \hat{p}_\gamma = 0$ for $\gamma \in (-\infty, k_s^2)$. Therefore, if the source is on the plane $x = 0$, at $(0, z_0)$, as in Eq. (1), we have for $x > 0$

$$\hat{p}(x,z) = \sum_{j=1}^{N} \frac{\hat{a}_{j,0}}{\sqrt{k_{zj}}} e^{ik_{zj}x}\phi_j(z) + \int_0^{k_s^2} \frac{\hat{a}_{\gamma,0}}{\gamma^{1/4}} e^{i\sqrt{\gamma}x}\phi_\gamma(z)d\gamma + \int_{-\infty}^{0} \frac{\hat{a}_{\gamma,0}}{|\gamma|^{1/4}} e^{-\sqrt{|\gamma|}x}\phi_\gamma(z)d\gamma, \tag{5}$$

with the mode amplitudes determined by the source

$$\hat{a}_{j,0} = \frac{\sqrt{k_{zj}}}{2}\phi_j(z_0), \quad j = 1, \ldots, N, \tag{6}$$

$$\hat{a}_{\gamma,0} = \frac{|\gamma|^{1/4}}{2}\phi_\gamma(z_0), \quad \gamma \in (-\infty, k_s^2). \tag{7}$$

IV. RANDOM AND DISSIPATIVE WAVEGUIDE

Here we assume that the waveguide is weakly randomly perturbed and weakly dissipative

$$c^2(x,z) = \frac{c_0^2(z)}{1+V(x,z)}. \tag{8}$$

The perturbation $V(x, z)$ has two components: random sound speed perturbation in water and deterministic constant dissipation in sediments

$$V(x,z) = \nu(x,z)\mathbf{1}_{(0,z_b)}(z) + i\nu_s\mathbf{1}_{(z_b,+\infty)}(z), \tag{9}$$

where $\nu(x, z)$ is a zero-mean random process that describes the relative fluctuations of the propagation speed in water, and $\nu_s > 0$ models the damping in the sediments. The random process ν is assumed to possess stationary and ergodic properties in the x-direction.[2,3,22] It is not, however, assumed to be delta-correlated in x. Indeed, we address a relatively high-frequency regime in which the correlation length of the medium is not smaller than the typical wavelength, so the delta correlation assumption is not fulfilled.

A. Coupled mode equations

The solution of the perturbed Helmholtz equation (1) for $x > 0$ can be expanded as Eq. (4), and the complex mode amplitudes satisfy the coupled equations[3]

$$\partial_x^2\hat{p}_j + k_{zj}^2\hat{p}_j = -\omega^2\sum_{l=1}^{N} C_{jl}(x)\hat{p}_l - \omega^2\int_{-\infty}^{k_s^2} C_{j\gamma'}(x)\hat{p}_{\gamma'}d\gamma', \tag{10}$$

for $j = 1, \ldots, N$,

$$\partial_x^2\hat{p}_\gamma + \gamma\hat{p}_\gamma = -\omega^2\sum_{l=1}^{N} C_{\gamma l}(x)\hat{p}_l - \omega^2\int_{-\infty}^{k_s^2} C_{\gamma\gamma'}(x)\hat{p}_{\gamma'}d\gamma', \tag{11}$$

for $\gamma \in (-\infty, k_s^2)$, with

$$C_{jl}(x) = \left(\phi_j, \phi_l V(x,\cdot)c_0^{-2}\right)_{L^2}, \tag{12}$$

and similar expressions for $C_{j\gamma'}$, $C_{\gamma l}$, and $C_{\gamma\gamma'}$. Here $(.,.)_{L^2}$ stands for the scalar product (A2). The coupling term C_{jl} has two components,

$$C_{jl}(x) = C_{jl}^{w}(x) + C_{jl}^{s}, \tag{13}$$

where

$$C_{jl}^{w}(x) = c_w^{-2}\rho_w^{-1}\int_0^{z_b}\nu(x,z)\phi_j(z)\phi_l(z)dz, \tag{14}$$

$$C_{jl}^{s} = i\nu_s\,\rho_s^{-1}c_s^{-2}\int_{z_b}^{+\infty}\phi_j(z)\phi_l(z)dz, \tag{15}$$

and similarly for the other coupling terms.

We introduce the amplitudes of the generalized right- and left-going mode amplitudes $\hat{a}_j$ and $\hat{b}_j$ for the guided and radiating modes defined by

$$\hat{a}_j(x) = \left(\frac{\sqrt{k_{zj}}}{2}\hat{p}_j(x) + \frac{1}{2i\sqrt{k_{zj}}}\partial_x\hat{p}_j(x)\right)e^{-ik_{zj}x}, \tag{16}$$

$$\hat{b}_j(x) = \left(\frac{\sqrt{k_{zj}}}{2}\hat{p}_j(x) - \frac{1}{2i\sqrt{k_{zj}}}\partial_x\hat{p}_j(x)\right)e^{ik_{zj}x}, \tag{17}$$

for $j = 1, \ldots, N$. They satisfy

$$\hat{p}_j(x) = \frac{1}{\sqrt{k_{zj}}}\left(\hat{a}_j(x)e^{ik_{zj}x} + \hat{b}_j(x)e^{-ik_{zj}x}\right), \tag{18}$$

$$\partial_x\hat{p}_j(x) = i\sqrt{k_{zj}}\left(\hat{a}_j(x)e^{ik_{zj}x} - \hat{b}_j(x)e^{-ik_{zj}x}\right), \tag{19}$$

for $j = 1, \ldots, N$. We define $\hat{a}_\gamma$ and $\hat{b}_\gamma$ similarly so that

$$\hat{p}_\gamma(x) = \frac{1}{\gamma^{1/4}}\left(\hat{a}_\gamma(x)e^{i\sqrt{\gamma}x} + \hat{b}_\gamma(x)e^{-i\sqrt{\gamma}x}\right), \tag{20}$$

$$\partial_x\hat{p}_\gamma(x) = i\gamma^{1/4}\left(\hat{a}_\gamma(x)e^{i\sqrt{\gamma}x} - \hat{b}_\gamma(x)e^{-i\sqrt{\gamma}x}\right), \tag{21}$$

for $\gamma \in (0, k_s^2)$. We say that $\hat{a}_j(x)$ is the generalized right-(left-)going mode amplitude, because it is the amplitude of the mode going into the positive (negative) x-direction. By differentiating Eqs. (16) and (17) with respect to x and using Eqs. (10), (11) and (18), (19), we find that the mode amplitudes satisfy the coupled differential equations

$$\begin{aligned}\partial_x\hat{a}_j = {} & \frac{i\omega^2 e^{-ik_{zj}x}}{2\sqrt{k_{zj}}} \\ & \times\left\{\sum_{l=1}^{N}\frac{C_{jl}(x)}{\sqrt{k_{zl}}}(\hat{a}_l(x)e^{ik_{zl}x} + \hat{b}_l(x)e^{-ik_{zl}x})\right. \\ & + \int_0^{k_s^2}\frac{C_{j\gamma'}(x)}{\sqrt{\gamma' 4}}(\hat{a}_{\gamma'}(x)e^{i\sqrt{\gamma'}x} + \hat{b}_{\gamma'}(x)e^{-i\sqrt{\gamma'}x})d\gamma' \\ & \left. + \int_{-\infty}^{0} C_{j\gamma'}(x)\hat{p}_{\gamma'}(x)d\gamma'\right\},\end{aligned} \tag{22}$$

$$\begin{aligned}\partial_x\hat{b}_j = {} & -\frac{i\omega^2 e^{ik_{zj}x}}{2\sqrt{k_{zj}}} \\ & \times\left\{\sum_{l=1}^{N}\frac{C_{jl}(x)}{\sqrt{k_{zl}}}(\hat{a}_l(x)e^{ik_{zl}x} + \hat{b}_l(x)e^{-ik_{zl}x})\right. \\ & + \int_0^{k_s^2}\frac{C_{j\gamma'}(x)}{\sqrt{\gamma' 4}}(\hat{a}_{\gamma'}(x)e^{i\sqrt{\gamma'}x} + \hat{b}_{\gamma'}(x)e^{-i\sqrt{\gamma'}x})d\gamma' \\ & \left. + \int_{-\infty}^{0} C_{j\gamma'}(x)\hat{p}_{\gamma'}(x)d\gamma'\right\}.\end{aligned} \tag{23}$$

The radiating mode amplitudes $\hat{a}_\gamma(x)$ and $\hat{b}_\gamma(x)$, $\gamma \in (0, k_s^2)$, satisfy the same equations upon replacing j by γ in the formulas above. The evanescent mode amplitudes $\hat{p}_\gamma(x)$, $\gamma \in (-\infty, 0)$, satisfy the differential equations

$$\partial_x^2 \hat{p}_\gamma + \gamma \hat{p}_\gamma = -g_\gamma(x) - \hat{g}_\gamma^{\mathrm{ev}}(x), \quad x \neq 0, \tag{24}$$

where $\hat{g}_\gamma(x)$ and $\hat{g}_\gamma^{\mathrm{ev}}(x)$ are given by

$$\hat{g}_\gamma(x) = \omega^2 \sum_{l'=1}^{N} \frac{C_{\gamma l'}(x)}{\sqrt{k_{zl'}}} \left[a_{l'}(x) e^{ik_{zl'}x} + b_{l'}(x) e^{-ik_{zl'}x}\right] + \omega^2 \int_0^{k_s^2} \frac{C_{\gamma\gamma'}(x)}{\sqrt{\gamma' 4}} \left[a_{\gamma'}(z) e^{i\sqrt{\gamma'}x} + b_{\gamma'}(x) e^{-i\sqrt{\gamma'}z}\right] d\gamma', \tag{25}$$

$$\hat{g}_\gamma^{\mathrm{ev}}(x) = \omega^2 \int_{-\infty}^{0} C_{\gamma\gamma'}(x) \hat{p}_{\gamma'}(x) d\gamma'. \tag{26}$$

B. Asymptotic analysis

We wish to understand the evolution of the complex mode amplitudes in the regime where the random sound speed perturbation in water and the seabed dissipation give rise to cumulative effects of the same order of magnitude. This is the most interesting and complete regime from the theoretical point of view, and also from the practical point of view, because the data set we deal with in Sec. V clearly reveals that both sound speed perturbations and seabed dissipation are significant. We use the multiscale analysis approach originally proposed in Ref. 3 and refined in Ref. 2, and we describe in this subsection the main steps. This approach requires quantifying the scaling ratios between the different physical parameters by the same dimensionless small parameter $\varepsilon > 0$. We consider the regime where the random perturbations are weak, of order ε, and dissipation is even weaker, of order ε^2. This choice of renormalization is the one for which the cumulative effects of both phenomena become of order one for long propagation distances, of order ε^{-2}, as we will see below. Therefore, in this section, we assume that the sound speed has the form (8) with

$$V(x,z) = \varepsilon \nu(x,z) \mathbf{1}_{z \in (0, z_b)} + i\varepsilon^2 \nu_s \mathbf{1}_{z \in (z_b, +\infty)}, \tag{27}$$

and that the waveguide is perfect (homogeneous and non-dissipative) outside the region $x \in (0, x_\infty/\varepsilon^2)$ for some $x_\infty > 0$. We carry out an asymptotic analysis in the small ε limit. In this framework, the evanescent mode amplitudes can be expressed in terms of the propagating mode amplitudes via Green's function of the Eq. (24).[2,23] The forward scattering approximation can be proved rigorously,[2] which makes it possible to decouple the a and b modes. The differential equation for $\hat{a}_j^\varepsilon(\omega, x) := \hat{a}_j(\omega, x/\varepsilon^2)$ can be written as

$$\partial_x \hat{a}_j^\varepsilon = \frac{i\omega^2}{2} \sum_{l=1}^{N} \frac{\frac{1}{\varepsilon} C_{jl}^{\mathrm{w}}\left(\frac{x}{\varepsilon^2}\right) + C_{jl}^{\mathrm{s}}}{\sqrt{k_{zj} k_{zl}}} \hat{a}_l^\varepsilon(x) e^{i(k_{zl} - k_{zj})(x/\varepsilon^2)} + \cdots.$$

Here, we write only the coupling terms with the guided mode amplitudes $\hat{a}_l^\varepsilon$, the "$\cdots$" contains the coupling terms (with similar forms) with $\hat{a}_{\gamma'}^\varepsilon$ [the second term on the right-hand side of Eq. (22)] and the coupling terms coming from the third term on the right-hand side of Eq. (22) and the expression of the evanescent modes $\hat{p}_{\gamma'}^\varepsilon$ in terms of the propagating ones. It is now clear that the scaling in Eq. (27) is such that the contributions of the seabed dissipation C_{jl}^{s} is of order 1, and the contributions of the zero-mean random sound speed perturbation in water appear in the form $(1/\varepsilon) C_{jl}^{\mathrm{w}}(x/\varepsilon^2)$, which give rise to effective terms of order one by diffusion approximation theory.[22] We deal with $\hat{a}_\gamma^\varepsilon(\omega, x) := \hat{a}_\gamma(\omega, x/\varepsilon^2)$ similarly. By taking the limit $\varepsilon \to 0$ as in Ref. 2, we can determine the asymptotic behavior of the complex guided and radiating mode amplitudes as expressed in Appendix B. The fourth remark in Appendix B shows that the process $(|\hat{a}_j^\varepsilon(x)|^2)_{j=1}^N$ (the vector of the guided mode powers) converges as $\varepsilon \to 0$ towards a Markov process $\boldsymbol{P}(x) = (P_j(x))_{j=1}^N$ whose generator is described below.

C. The effective Markovian dynamics of the mode powers

From Sec. IV B, in the regime of interest for this paper, the effective dynamics of the vector of the guided mode powers $\boldsymbol{P}(x) = (P_j(x))_{j=1}^N$,

$$P_j(x) = |\hat{a}_j(x)|^2, \tag{28}$$

is Markovian with infinitesimal generator $\mathcal{L}_{\boldsymbol{P}}$,

$$\mathcal{L}_{\boldsymbol{P}} = \sum_{j \neq l} \Gamma_{lj} \left[P_l P_j (\partial_{P_j} - \partial_{P_l}) \partial_{P_j} + (P_l - P_j) \partial_{P_j}\right] - \sum_{j=1}^{N} \Lambda_j P_j \partial_{P_j}, \tag{29}$$

with

$$\Gamma_{lj} = \frac{\omega^4}{2 k_{zj} k_{zl}} \int_0^\infty \mathcal{R}_{jl}^{\mathrm{w}}(x) \cos\left((k_{zl} - k_{zj})x\right) dx, \tag{30}$$

$$\Lambda_j = \int_0^{k_s^2} \frac{\omega^4}{2\sqrt{\gamma} k_{zj}} \int_0^\infty \mathrm{R}_{j\gamma}^{w}(x) \cos\left((\gamma - k_{zj})x\right) dx d\gamma + \nu_s \frac{\omega^4}{k_{zj} c_s^2 \rho_s} \int_{z_b}^\infty \phi_j(z)^2 dz, \tag{31}$$

for $j \neq l$, where

$$\mathcal{R}_{jl}^{\mathrm{w}}(x) := \mathbb{E}\left[C_{jl}^{\mathrm{w}}(0) C_{jl}^{\mathrm{w}}(x)\right] = \rho_{\mathrm{w}}^{-2} c_{\mathrm{w}}^{-4} \times \int_0^{z_b} \int_0^{z_b} \phi_j \phi_l(z) \mathbb{E}\left[\nu(0,z)\nu(x,z')\right] \phi_j \phi_l(z') dz dz', \tag{32}$$

and similarly for $\mathcal{R}_{j\gamma}^{\mathrm{w}}(x) = \mathbb{E}[C_{j\gamma}^{\mathrm{w}}(0) C_{j\gamma}^{\mathrm{w}}(x)]$.

This means that, for any test function $F : \mathbb{R}^N \to \mathbb{R}$, the expectation $\mathbb{E}[F(\boldsymbol{P}(x))]$ satisfies the Kolmogorov forward equation[22]

$$\partial_x \mathbb{E}[F(\boldsymbol{P}(x))] = \mathbb{E}[\mathcal{L}_{\boldsymbol{P}} F(\boldsymbol{P}(x))], \tag{33}$$

which makes it possible to compute any moment of the mode powers.

The coefficients Γ_{jl} describe the effective mode coupling between guided modes due to random sound speed. The coefficients Λ_j are effective mode-dependent damping factors and have two contributions: the first contribution in Eq. (31) comes from the coupling between guided and radiative modes due to random sound speed; the second contributions in Eq. (31) come from the attenuation in the sediments.

From the form of the generator $\mathcal{L}_{\boldsymbol{P}}$, one can establish that the nth-order moments of the mode powers satisfy closed equations. We will apply this to the first moment of $\boldsymbol{P}$, as well as its second moment later in Sec. IV G.

Using Eqs. (29) and (33) with $F(\boldsymbol{P}) = P_j$, we find that the mean mode powers

$$Q_j(x) = \mathbb{E}\big[P_j(x)\big] = \mathbb{E}\Big[|\hat{a}_j(x)|^2\Big] \tag{34}$$

satisfy the closed system of equations

$$\partial_x Q_j = -\Lambda_j Q_j + \sum_{l=1}^{N} \Gamma_{lj}(Q_l - Q_j), \tag{35}$$

starting from $Q_j(0) = |\hat{a}_{j,0}|^2$. The form of these coupled-mode equations is well-known;[9] although the mode-dependent attenuation term Λ_j was thus far introduced only heuristically. The solution is explicitly written as

$$\boldsymbol{Q}(x) = \exp(\mathbf{A}x)\boldsymbol{Q}(0), \tag{36}$$

with the matrix $\mathbf{A}$ defined by (δ_{jl} is the Kronecker symbol and $\Gamma_{jj} = -\sum_{l' \neq j} \Gamma_{jl'}$)

$$\mathbf{A} := (\Gamma_{jl} - \Lambda_j \delta_{jl})_{j,l=1}^{N}. \tag{37}$$

D. Computation of the coefficients of matrix A

The goal of this section is to show how to get closed-form expressions of the coefficients of matrix $\mathbf{A}$ when the correlation of the perturbation decreases exponentially as a function of the horizontal distance between the two points, i.e.,

$$\mathbb{E}\big[\nu(x,z)\nu(x',z')\big] = \sigma^2 \exp(-|x-x'|/\ell_{\mathrm{h}}) R(z,z'), \tag{38}$$

where ℓ_{h} is the horizontal correlation radius of the random fluctuations of the index of refraction, and R is the vertical correlation function of the perturbation. By substituting Eq. (38) into Eq. (32), we obtain

$$\begin{aligned}\int_0^{\infty} \mathcal{R}^{\mathrm{w}}_{jl}(x) \cos\big((k_{zl} - k_{zj})x\big)dx \\ = \frac{\sigma^2 \rho_{\mathrm{w}}^{-2} c_{\mathrm{w}}^{-4} \ell_{\mathrm{h}}}{1 + (k_{zl} - k_{zj})^2 \ell_{\mathrm{h}}^2} \\ \times \int_0^{z_{\mathrm{b}}} \int_0^{z_{\mathrm{b}}} R(z,z')\phi_j\phi_l(z)\phi_j\phi_l(z')dzdz',\end{aligned} \tag{39}$$

which gives with Eq. (30) the following expression of Γ_{jl}:

$$\begin{aligned}\Gamma_{jl} = \frac{\omega^4}{2k_{zj}k_{zl}} \frac{\sigma^2 \rho_{\mathrm{w}}^{-2} c_{\mathrm{w}}^{-4} \ell_{\mathrm{h}}}{1 + (k_{zl} - k_{zj})^2 \ell_{\mathrm{h}}^2} \\ \times \int_0^{z_{\mathrm{b}}} \int_0^{z_{\mathrm{b}}} R(z,z')\phi_j\phi_l(z)\phi_j\phi_l(z')dzdz'\end{aligned} \tag{40}$$

for $j \neq l$. Similarly, we can compute Λ_j from the same quantities upon substituting γ for l. Replacing ϕ_j for all j by their expression, and using the notation $k_j^{\mathrm{w}} := \sqrt{k_{\mathrm{w}}^2 - k_{zj}^2}$, we obtain

$$\begin{aligned}\int_0^{z_{\mathrm{b}}} \int_0^{z_{\mathrm{b}}} R(z,z')\phi_j\phi_l(z)\phi_j\phi_l(z')dzdz' \\ = \frac{\chi_j^2 \chi_l^2}{4}\Big(S(k_j^{\mathrm{w}} - k_l^{\mathrm{w}}, k_j^{\mathrm{w}} - k_l^{\mathrm{w}}) + S(k_j^{\mathrm{w}} + k_l^{\mathrm{w}}, k_j^{\mathrm{w}} + k_l^{\mathrm{w}}) \\ - S(k_j^{\mathrm{w}} - k_l^{\mathrm{w}}, k_j^{\mathrm{w}} + k_l^{\mathrm{w}}) - S(k_j^{\mathrm{w}} + k_l^{\mathrm{w}}, k_j^{\mathrm{w}} - k_l^{\mathrm{w}})\Big),\end{aligned} \tag{41}$$

where

$$S(k,k') := \int_0^{z_{\mathrm{b}}} \int_0^{z_{\mathrm{b}}} R(z,z') \cos(kz) \cos(k'z')dzdz'. \tag{42}$$

When R has the exponential form $R(z,z') = \exp(-|z-z'|/\ell_{\mathrm{v}})/2$, where ℓ_{v} is the vertical correlation radius of the random fluctuations of the index of refraction, then the relative variance of the fluctuations is $\sigma^2/2$, and $S(k,k')$ has a closed-form expression. We use this particular form of the correlation function of the medium in Sec. V, because it gives simple expressions for the coefficients Γ_{jl} and Λ_j. This is convenient for the resolution of the inverse problem, which requires many evaluations of such coefficients for different values σ, ℓ_{v}, ℓ_{h} of the statistics of the random medium and ρ_{s}, ν_{s} of the sea bottom. We could as well use the Garrett–Munk correlation function at the expense of some computational overburden,[24] but the impact of the exact form of the correlation function turns out to be negligible.

E. Pressure field correlations

We now compute the correlation of the received signal on a vertical segment at a fixed horizontal distance x_{a}. When $x_{\mathrm{a}} \gg 1$, we can use the asymptotic study from above, and the decomposition of $\hat{p}(x_{\mathrm{a}}, z)$ is

$$\hat{p}(x_{\mathrm{a}}, z) \simeq \sum_{j=1}^{N} \frac{1}{\sqrt{k_{zj}}} \hat{a}_j(x_{\mathrm{a}})\phi_j(z)e^{ik_{zj}x_{\mathrm{a}}}. \tag{43}$$

Here, we do not write the contributions of the radiating modes or the evanescent modes, which are much smaller inside the water column. Therefore,

$$\begin{aligned}\mathbb{E}\Big[\overline{\hat{p}(x_{\mathrm{a}}, z)}\hat{p}(x_{\mathrm{a}}, z')\Big] \\ = \sum_{j=1}^{N} \frac{\mathbb{E}\Big[|\hat{a}_j(x_{\mathrm{a}})|^2\Big]}{k_{zj}} \phi_j(z)\phi_j(z') \\ + \sum_{j \neq l} \frac{\mathbb{E}\Big[\overline{\hat{a}_j(x_{\mathrm{a}})}\hat{a}_l(x_{\mathrm{a}})\Big]}{\sqrt{k_{zj}k_{zl}}} \phi_j(z)\phi_l(z')e^{i(k_{zj} - k_{zl})x_{\mathrm{a}}}.\end{aligned} \tag{44}$$

The cross second moments $\mathbb{E}[\overline{\hat{a}_j}\hat{a}_l]$ for $j \neq l$ decay exponentially with the propagation distance x as shown in Ref. 1 (see also Ref. 7), and they can be neglected as soon as the propagation distance x is larger than the scattering mean free path that depends on the coefficients Γ_{jl}. Roughly speaking, this is the distance beyond which the phase of the field has a random part whose variance is on the order of or larger than one, so that the coherent field is vanishing.[1,4] The second moments $\mathbb{E}[|\hat{a}_j|^2]$ were computed in the previous paragraph using the exponential of matrix $\mathbf{A}$,

$$\mathbb{E}\left[|\hat{a}_j(x_a)|^2\right] = \sum_{l=1}^{N} (\exp(\mathbf{A}x_a))_{jl} |\hat{a}_{l,0}|^2, \tag{45}$$

where $\hat{a}_{l,0}$ is given by Eq. (6). We can now write the correlation between the sound pressure signals recorded by two receivers, which are separated by y along the vertical segment at distance x_a and of depth $[z_m, z_M]$; where $0 < z_m < z_M < z_b$. For all $y \in [0, z_M - z_m]$, the spatial correlation $C_{x_a}(y)$ is written as

$$\begin{aligned} C_{x_a}(y) :&= \frac{1}{z_M - z_m - y} \int_{z_m}^{z_M - y} \mathbb{E}\left[\overline{\hat{p}(x_a, z)} \hat{p}(x_a, z + y)\right] dz \\ &= \frac{1}{z_M - z_m - y} \sum_{j=1}^{N} \frac{\mathbb{E}\left[|\hat{a}_j(x_a)|^2\right]}{k_{zj}} \frac{\chi_j^2}{2} \\ &\quad \times \Bigg(\cos(k_{wj} y)(z_M - z_m - y) \\ &\quad - \frac{\sin(k_{wj}(2z_M - y)) - \sin(k_{wj}(2z_m + y))}{2k_{wj}} \Bigg). \end{aligned} \tag{46}$$

F. Equipartition regime

By (36) the mean mode powers satisfy

$$Q_j(x) \overset{x \to +\infty}{\simeq} c_V V_j \exp(-\lambda x)(1 + o(1)),$$

where $(\boldsymbol{V}, -\lambda)$ is the first eigenvector/eigenvalue of matrix $\mathbf{A} = \mathbf{\Gamma} - \mathbf{\Phi}$, with Γ_{jl} given by (30) for $j \neq l$, $\Gamma_{jj} = -\sum_{l' \neq j} \Gamma_{jl'}$, $\Phi_{jl} = \Lambda_j \delta_{jl}$, and

$$c_V = \sum_{l=1}^{N} V_l |\hat{a}_{l,0}|^2.$$

By using classical Perron–Frobenius arguments[25] one can get information about the spectrum of $\mathbf{A}$: First, the coefficients of $\boldsymbol{V}$ have all the same sign (so we can assume that they are nonnegative). Second, the eigenvalue $-\lambda$ is simple and $\lambda \geq 0$.

In the following, we discuss cases with zero or weak dissipation, where explicit expressions can be obtained. Remember that the effective dissipation is the sum of two effects: power leakage from the guided modes to the radiating modes and dissipation in the sediments.

1. No effective dissipation

If there is no effective dissipation $\mathbf{\Phi} = \mathbf{0}$, then the first eigenvector/eigenvalue $(\boldsymbol{V}^{(0)}, -\lambda^{(0)})$ of the matrix $\mathbf{\Gamma}$ is

$$\boldsymbol{V}^{(0)} = \left(1/\sqrt{N}\right)_{j=1}^{N}, \quad \lambda^{(0)} = 0,$$

which gives the standard equipartition result[1,8,22]

$$Q_j(x) \xrightarrow{x \to +\infty} \frac{1}{N} \sum_{l=1}^{N} |\hat{a}_{l,0}|^2.$$

The total input energy $\sum_{l=1}^{N} |\hat{a}_{l,0}|^2$ becomes equipartitioned amongst all propagating modes.

2. Weak effective dissipation

We next consider the case when the effective dissipation is weak, that is to say, the matrix $\mathbf{\Phi}$ is much smaller than the matrix $\mathbf{\Gamma}$, with a typical ratio on the order of the small dimensionless parameter $\delta \ll 1$. We then assume that $\Lambda_j = \delta \Lambda_j^{(1)}$. Then we can write $\mathbf{\Phi} = \delta \mathbf{\Phi}^{(1)}$ with $\Phi_{jl}^{(1)} = \Lambda_j^{(1)} \delta_{jl}$ and $\mathbf{\Gamma} = \mathbf{\Gamma}^{(0)}$, and the first eigenvector/eigenvalue $(\boldsymbol{V}, -\lambda)$ of the matrix $\mathbf{\Gamma} - \mathbf{\Phi}$ can be expanded as

$$\boldsymbol{V} = \boldsymbol{V}^{(0)} + \delta \boldsymbol{V}^{(1)} + O(\delta^2), \quad \lambda = \delta \lambda^{(1)} + \delta^2 \lambda^{(2)} + O(\delta^3),$$

with

$$\lambda^{(1)} = \boldsymbol{V}^{(0)T} \mathbf{\Phi}^{(1)} \boldsymbol{V}^{(0)} = \frac{1}{N} \sum_{j=1}^{N} \Lambda_j^{(1)}, \tag{47}$$

$$\lambda^{(2)} = \boldsymbol{V}^{(0)T} \Gamma^{(0)} \boldsymbol{V}^{(1)}, \tag{48}$$

and $\boldsymbol{V}^{(1)}$ is a solution to $\Gamma^{(0)} \boldsymbol{V}^{(1)} = (\Phi^{(1)} - \lambda^{(1)}) \boldsymbol{V}^{(0)}$ and is orthogonal to $\boldsymbol{V}^{(0)}$. If, for instance, $\Gamma_{jl} \equiv \Gamma > 0$ for all $j \neq l$, then $\boldsymbol{V}^{(1)} = -[1/(\Gamma N^{3/2})](\Lambda_j^{(1)})_{j=1}^{N}$ and

$$\lambda^{(2)} = -\frac{1}{\Gamma N^2} \sum_{j=1}^{N} (\Lambda_j^{(1)} - \lambda^{(1)})^2.$$

G. Fluctuation analysis

By Eq. (29), we find that the second-order moments of the mode powers

$$R_{jl}(x) = \mathbb{E}\left[P_j(x) P_l(x)\right], \quad j, l = 1, \ldots, N, \tag{49}$$

satisfy the closed equations

$$\partial_x R_{jj} = -2\Lambda_j R_{jj} + \sum_{n \neq j} \Gamma_{jn} (4R_{jn} - 2R_{jj}), \tag{50}$$

$$\begin{aligned} \partial_x R_{jl} = &-(2\Gamma_{jl} + \Lambda_j + \Lambda_l) R_{jl} + \sum_{n \neq l} \Gamma_{ln} (R_{jn} - R_{jl}) \\ &+ \sum_{n \neq j} \Gamma_{jn} (R_{nl} - R_{jl}), \end{aligned} \tag{51}$$

for $j \neq l$. This system has the same form as the one found in the literature dedicated to coupled mode theory.[8,9] The initial conditions are $R_{jl}(0) = |\hat{a}_{j,0}|^2 |\hat{a}_{l,0}|^2$. Let us introduce $\boldsymbol{S} = (S_{jl})_{1 \leq j \leq l \leq N}$ defined by

$$S_{jl} = \begin{cases} R_{jl} + R_{lj} & \text{if } j < l, \\ R_{jj} & \text{if } j = l. \end{cases} \tag{52}$$

The S_{jl}'s satisfy the system

$$\partial_x S_{jl} = -(\Lambda_j + \Lambda_l) S_{jl} + 2\Gamma_{jl} 1_{j\neq l}(S_{jj} + S_{ll} - 2S_{jl}) + \sum_{n\notin\{j,l\}} \left[\Gamma_{ln}(S_{jn} - S_{jl}) + \Gamma_{jn}(S_{nl} - S_{jl})\right], \tag{53}$$

with the convention that whenever S_{jl} occurs with $j > l$, it is replaced by S_{lj}. This can be written in the form $\partial_x \boldsymbol{S} = (\boldsymbol{\Theta} - \boldsymbol{\Psi})\boldsymbol{S}$. The linear operator $\boldsymbol{\Psi}$ (that depends on the Λ_j's) is diagonal, and the linear operator Θ (that depends on Γ_{jl}'s) is self-adjoint: for any $\boldsymbol{T}$ and $\tilde{\boldsymbol{T}}$, we have $\sum_{j\le l}(\boldsymbol{\Theta T})_{jl}\tilde{T}_{jl} = \sum_{j\le l} T_{jl}(\boldsymbol{\Theta}\tilde{\boldsymbol{T}})_{jl}$. As a consequence, $\boldsymbol{\Phi} - \boldsymbol{\Psi}$ can be diagonalized, and we find that

$$\boldsymbol{S}(x) \overset{x\to+\infty}{\simeq} c_W \boldsymbol{W} \exp(-\mu x)(1 + o(1)),$$

where c_W is the projection on the first eigenvector $\boldsymbol{W}$ on the basis of eigenvectors of $\boldsymbol{\Phi} - \boldsymbol{\Psi}$, $-\mu$ is the first eigenvalue, and

$$c_W = \sum_{j,l=1}^{N} W_{jl} |\hat{a}_{j,0}|^2 |\hat{a}_{l,0}|^2,$$

with the convention that whenever W_{jl} occurs with $j > l$, it is replaced by W_{lj}.

1. No effective dissipation

If there is no effective dissipation, then the first eigenvector/eigenvalue $(\boldsymbol{W}^{(0)}, -\mu^{(0)})$ of the matrix $\boldsymbol{\Theta}$ is $\boldsymbol{W}^{(0)} = (c_N)_{1\le j\le l\le N}$, $\mu^{(0)} = 0$, with $c_N = \sqrt{2}/\sqrt{N(N+1)}$. We have $\boldsymbol{S}(x) \overset{x\to+\infty}{\to} c_W \boldsymbol{W}^{(0)}$. As $\sum_{j\le l} S_{jl}(x) = \sum_{j,l} R_{jl}(x) = (\sum_{j=1}^{N} |\hat{a}_{j,0}|^2)^2$, we deduce that, for any j, l,

$$R_{jl}(x) \overset{x\to+\infty}{\longrightarrow} \left(\sum_{l'=1}^{N} |\hat{a}_{l',0}|^2\right)^2 \frac{1 + \delta_{jl}}{N(N+1)}.$$

This means that, when $N \gg 1$, the mode powers P_j become uncorrelated and their marginal distributions have the same moments as exponential distributions. In other words, the mode powers behave as the square moduli of independent and identically distributed complex Gaussian variables.

2. Weak effective dissipation

We next consider the case when the effective dissipation is weak, say $\Lambda_j = \delta\Lambda_j^{(1)}$ with $\delta \ll 1$. Then we can write $\boldsymbol{\Psi} = \delta\boldsymbol{\Psi}^{(1)}$ and $\boldsymbol{\Theta} = \boldsymbol{\Theta}^{(0)}$, and the first eigenvector/eigenvalue $(\boldsymbol{W}, -\mu)$ of the matrix $\boldsymbol{\Theta} - \boldsymbol{\Psi}$ can be expanded as

$$\boldsymbol{W} = \boldsymbol{W}^{(0)} + \delta\boldsymbol{W}^{(1)} + O(\delta^2), \quad \mu = \delta\mu^{(1)} + \delta^2\mu^{(2)} + O(\delta^3),$$

with

$$\mu^{(1)} = \boldsymbol{W}^{(0)T}\boldsymbol{\Psi}^{(1)}\boldsymbol{W}^{(0)} = \frac{2}{N}\sum_{j=1}^{N}\Lambda_j^{(1)} = 2\lambda^{(1)},$$
$$\mu^{(2)} = \boldsymbol{W}^{(1)T}\boldsymbol{\Theta}^{(0)}\boldsymbol{W}^{(1)}, \tag{54}$$

and $\boldsymbol{W}^{(1)}$ is a solution to $\boldsymbol{\Theta}^{(0)}\boldsymbol{W}^{(1)} = (\boldsymbol{\Psi}^{(1)} - \mu^{(1)})\boldsymbol{W}^{(0)}$ and is orthogonal to $\boldsymbol{W}^{(0)}$. If, for instance, $\Gamma_{jl} \equiv \Gamma > 0$ for all $j \neq l$, then

$$W_{jl}^{(1)} = -\frac{c_N}{\Gamma N}\left(\Lambda_j^{(1)} + \Lambda_l^{(1)} - 2\lambda^{(1)}\right), \quad j \le l,$$

and

$$\mu^{(2)} = \sum_{j\le l} W_{jl}^{(1)}(\boldsymbol{\Theta}^{(0)}\boldsymbol{W}^{(1)})_{jl} = -\frac{2(N+2)}{N^2(N+1)\Gamma}\sum_{j=1}^{N}(\Lambda_j^{(1)} - \lambda^{(1)})^2.$$

Note that

$$\mu - 2\lambda = \delta^2\left(\mu^{(2)} - 2\lambda^{(2)}\right) + O(\delta^3) = -\frac{2\delta^2}{N^2(N+1)\Gamma}\sum_{j=1}^{N}(\Lambda_j^{(1)} - \lambda^{(1)})^2 + O(\delta^3) \tag{55}$$

is negative-valued.

3. Exponential growth of the intensity fluctuations

It is a general feature that, for any matrix Γ and effective dissipation coefficients Λ_j, we have $\mu - 2\lambda \le 0$ [we have equality when there is no effective dissipation, a consequence of the forthcoming result (58) and Cauchy–Schwarz inequality when there is dissipation]. The first two moments of the pointwise intensity $|\hat{p}(x,z)|^2$ for large x are

$$\mathbb{E}\left[|\hat{p}(x,z)|^2\right] = \sum_{j=1}^{N}\frac{\phi_j(z)^2}{k_{zj}} c_V V_j e^{-\lambda x}, \tag{56}$$

$$\mathbb{E}\left[|\hat{p}(x,z)|^4\right] = \sum_{j,l=1}^{N}\frac{\phi_j(z)^2\phi_l(z)^2}{k_{zj}k_{zl}} c_W W_{jl} e^{-\mu x}. \tag{57}$$

Without dissipation, we have the following result for the fluctuations of the pointwise intensity:

$$\frac{\mathbb{E}\left[|\hat{p}(x,z)|^4\right]}{\mathbb{E}\left[|\hat{p}(x,z)|^2\right]^2} \xrightarrow{x\to\infty} \frac{2N}{N+1},$$

which is equal to 2 when $N \gg 1$, and with weak dissipation

$$\frac{\mathbb{E}\left[|\hat{p}(x,z)|^4\right]}{\mathbb{E}\left[|\hat{p}(x,z)|^2\right]^2} \overset{x\to\infty}{\simeq} \frac{2N}{N+1}\exp(-(\mu - 2\lambda)x), \tag{58}$$

which grows exponentially with the propagation distance (for very long distances, however, as $|\mu - 2\lambda|$ is very small,

as shown above). Equation (55) gives the expression of the exponential growth rate when dissipation is weak and $\Gamma_{jl} \equiv \Gamma$ for $j \neq l$: the growth rate increases when the effective modal dissipation coefficients become different from each other and decreases when the number of modes increases.

V. INVERSE PROBLEM

The goal of this section is to show that it is possible to estimate the statistical properties of the index of refraction in the water column and the sea bottom properties from the incoherent sound pressure recorded by a vertical hydrophone array and transmitted by distant time-harmonic sources. This inverse problem can be formulated as a minimization problem that tries to match empirical quantities with theoretical ones that depend on the parameters to be estimated. The theoretical model of the Sec. IV shows that the correlation function of the sound pressure has a non-trivial behavior that makes it possible to identify many relevant parameters, as we will explain below. We first present the ALMA experimental data, then formulate the inverse problem, and finally estimate the model parameters.

A. ALMA 2016 experiment

ALMA is a series of at-sea experiments carried out by the French DGA Naval Systems.[20] In 2016, the experiment took place from November 7–17 near the shores of North East Corsica[26] (cf. Fig. 1). There is a moored pinger at the $z_0 = 50$ m immersion depth and a passive array with 128 hydrophones at the 60 m immersion depth. More exactly, the array consists of 4 vertical arms of 32 hydrophones. The arms are 0.5 m apart from each other, and for each vertical arm the hydrophones are regularly spaced between the depths $z_m = 58.35$ m and $z_M = 63$ m, at 0.15 m apart from each other. The distance between the source and the array is $x_a = 9000$ m. The sea bottom is relatively flat on the line between the pinger and the array (the bottom depth is somewhere between 100 and 115 m) but sloppy on the orthogonal direction. Seafloor is composed of sand and gravelly sand. The sea was calm, with a roughness height around 0.1 m (sea state 1). The pinger transmitted, for a period of approximately 2.5 h, a sequence consisting of several time-harmonic waves, with a repetition rate of three minutes. The sequence is a train of two-second time-harmonic waves, at the following $K = 6$ frequencies: 2, 5, 7, 9, 11, and 13 kHz. Acquisition is sampled at 48 kHz. The Fourier coefficients for each frequency are extracted using a Hann window function with a duration of 1 s. This gives 50 time samples by frequency.

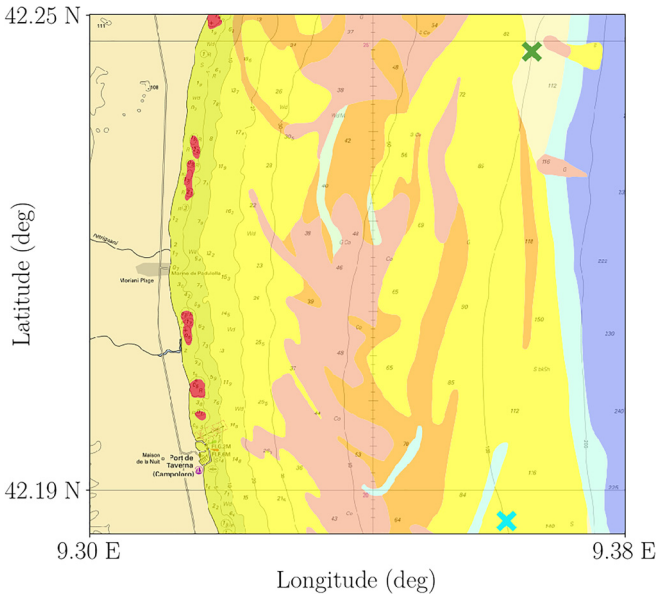

FIG. 1. (Color online) Top view of the experimental setup measurements region (source: Ref. 30); the blue cross (bottom right) is the source (42°19.656 N 9°37.004E); the green cross (top right) is the receiver array (42°24.693 N 9°37.363E); yellow region: sand sediment; orange region: gravelly sand sediment. The bathymetry contour line that goes through the crosses is 100 m. The one on the right (left) of the crosses is 200 m (50 m).

At frequency ω, for $y \in [0, z_M - z_m]$, we denote the spatial correlation between the signals recorded by two hydrophones at a distance y from each other by $C_{x_a}(y)$ [cf. Eqs. (45) and (46) for the theoretical expression predicted by our model]. Then we define the correlation radius r as the half-width at half-maximum (i.e., the distance between hydrophones for which the correlation is 1/2)

$$C_{x_a}(r) = \frac{1}{2} C_{x_a}(0) = \frac{1}{2}. \tag{59}$$

From the experimental data at frequencies $f_1, \ldots, f_K$ (with $\omega = 2\pi f$), we extract the experimental correlation radii $r_e(f_1), \ldots, r_e(f_K)$. For $\Phi = (c_s, \rho_s, \nu_s, \sigma, \ell_v, \ell_h)$, a set of parameters of our theoretical model (assuming that we know the sound speed c_w and density ρ_w in water and the depth of the sea bottom), we compute the theoretical correlation radii $r_t(f_1, \Phi), \ldots, r_t(f_K, \Phi)$. Then we define the misfit function

$$E(\Phi) = \sum_{k=1}^{K} \left(r_t(f_k, \Phi) - r_e(f_k)\right)^2, \tag{60}$$

and we determine the parameters Φ by minimizing over Φ the misfit function $E(\Phi)$ (by the L-BFGS-B algorithm[27]).

B. Estimation of the model parameters

We assume that sound speed is constant in water, taking value $c_w = 1523$ m/s from CTD (conductivity, temperature, and depth) measurements, and we set the density of water

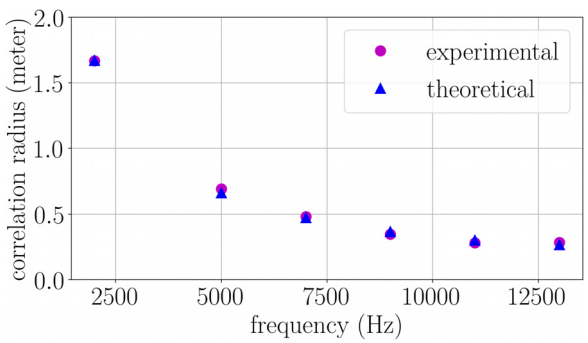

FIG. 2. (Color online) Comparisons between experimental and theoretical correlation radii.

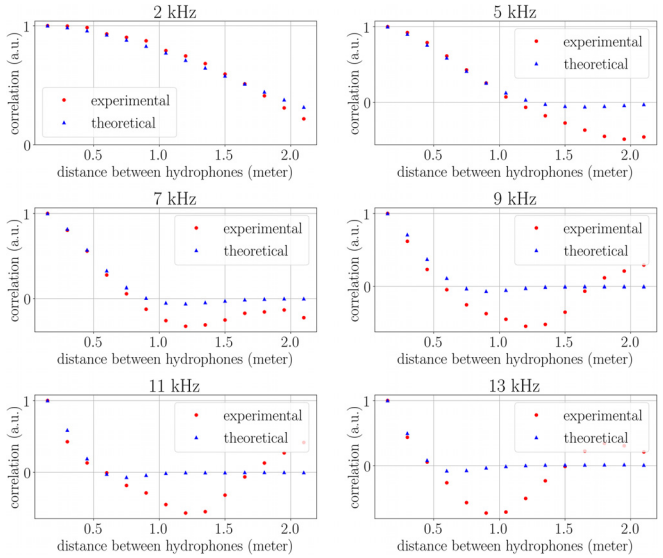

FIG. 3. (Color online) Experimental and theoretical correlation functions at different frequencies.

ρ_w at 1000 kg/m^3 (we could have taken a more precise value, but density has little influence on the model). Figure 2 presents the correlation radii obtained from experimental data for each frequency, and the theoretical correlation radii predicted by our model with the parameters determined by minimization of the misfit function (60): $c_s = 1599$ m/s; $\alpha = 1.51$ dB/wavelength; $\sigma = 0.0030$ ($\sigma^2/2$=relative variance); $\ell_v = 12.1$ m; $\ell_h = 100$ m; $\rho_s = 1700$ kg/m^3. Parameter ν_s is computed from the attenuation coefficient α expressed in decibels by wavelength. The values of the parameters seem compatible with experimental measurements carried out in similar environments.[28] Figure 3 shows theoretical and experimental correlation functions at the different frequencies. The empirical correlation functions at large offsets are noisy because there are a limited number of samples for these large offsets.

We carry out a global sensitivity analysis by computing first-order and total Sobol indices[29] of the theoretical correlation radii r_t (f_k, Φ) based on the expressions (45) and (46) as functions of the six parameters $\Phi = (c_s, \rho_s, \alpha, \sigma, \ell_v, \ell_h)$ (following the uniform distribution on the hypercube $[1530, 1630] \times [1650, 1750] \times [0.5, 2.0] \times [0, 0.005] \times [5, 50] \times [50, 150]$, that encompasses the physical data reported in Ref. 28). We can see in Fig. 4 that the two most important parameters are c_s and σ, that α and ℓ_v have less influence, but are still significant. Finally, ρ_s and ℓ_h have no noticeable effect, whatever the frequency. We can also quantify the uncertainty in the parameter estimation by a Bayesian analysis. The *a priori* distribution is the uniform distribution on the hypercube. The

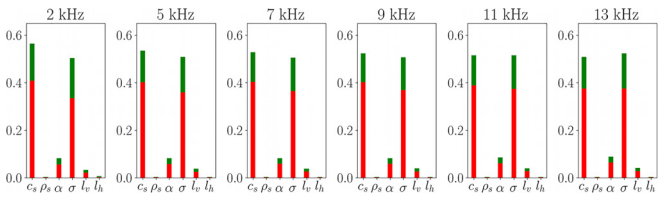

FIG. 4. (Color online) First-order (red) and total (green) Sobol indices of the theoretical correlation radii as functions of c_s, ρ_s, α, σ, ℓ_v, and ℓ_h.

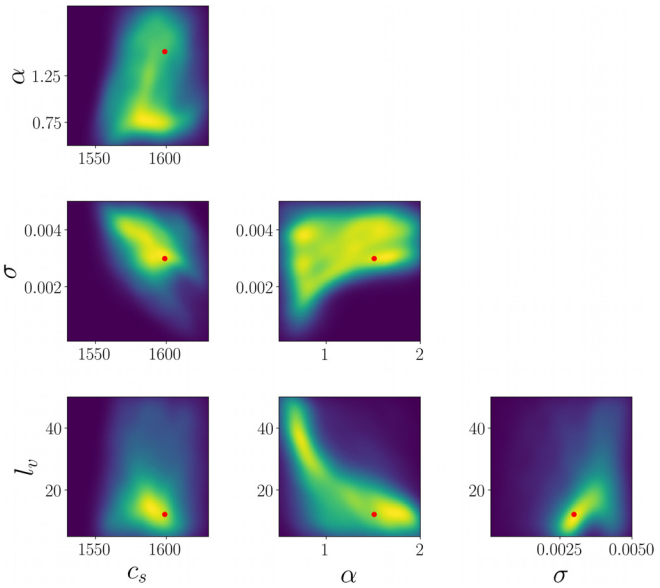

FIG. 5. (Color online) *A posteriori* distribution of the four parameters c_s (in *m/s*), α (in *dB*/wavelength), σ, and ℓ_v (in *m*). Two-dimensional marginal distributions are plotted for all pairs of parameters. The red point is the maximum *a posteriori* estimator, that is, the minimum of the misfit function (60).

likelihood is obtained by assuming that the errors in the experimental correlation radii are independent, Gaussian, with the same variance. The variance is obtained from the residuals evaluated for the optimal Φ minimizing the misfit function (60). The *a posteriori* distribution of the parameters ρ_s and ℓ_h is the *a priori* one (uniform), because the theoretical model is not sensitive to these parameters. In Fig. 5 we plot the four-dimensional *a posteriori* distribution of (σ, α, c_s, ℓ_v). We can see *a posteriori* correlations between σ, ℓ_v, and α, which may make them difficult to identify individually.

The inspection of the numerical values of the two terms that determine Λ_j [cf. Eq. (31)] give interesting information. We can see that for each frequency, the radiative contributions are approximately one thousand times smaller than the attenuation ones. In the experimental configuration addressed in this paper, we can claim that radiation effects can be neglected.

Finally, if we denote by $(z_n)_{1 \leqslant n \leqslant N_h}$ the depths of the N_h hydrophones of the array, we can compare the theoretical, frequency-dependent the scintillation indices defined by

$$S_t = \frac{1}{N_h} \sum_{n=1}^{N_h} \frac{\mathbb{E}\left[|\hat{p}(x_a, z_n)|^4\right] - \mathbb{E}\left[|\hat{p}(x_a, z_n)|^2\right]^2}{\mathbb{E}\left[|\hat{p}(x_a, z_n)|^2\right]^2}, \qquad (61)$$

with the experimental values S_e determined by empirical averages instead of expectations. Table I shows experimental scintillation indices compared to theoretical ones, with the optimal parameters Φ determined from the correlation radii. In

TABLE I. Experimental and theoretical scintillation indices at different frequencies.

	2 kHz	5 kHz	7 kHz	9 kHz	11 kHz	13 kHz
Experiment	0.82	0.89	1.06	1.41	1.16	1.89
Theory	0.97	0.99	0.99	0.99	0.99	0.99

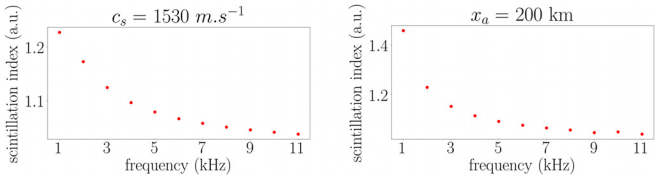

FIG. 6. (Color online) Scintillation indices when $c_s = 1530$ m/s (left) or when the propagation distance $x_a = 200$ km (right).

the experimental and theoretical configurations scintillation indices are approximately equal to one. One should have longer propagation distances to observe scintillation indices larger than one, as suggested in Ref. 8. We report in Fig. 6 the scintillation indices when the propagation distance is large ($x_a = 200$ km) or when the sound speed mismatch between the water column and the sediments is small ($c_s = 1530$ m/s). In these cases, the scintillation indices are significantly larger than one. In the case of a large propagation distance, this can be understood by the fact that the scintillation index grows exponentially with the propagation distance. In the case of small sound speed mismatch, this can be explained by the fact that the waveguide then supports a small number of propagating modes and we have shown that the growth rate increases when the number of modes decreases.

VI. CONCLUSION

This paper proposes a complete description of the statistics of the mode amplitudes of the sound pressure in a shallow-water waveguide. The effective parameters (frequency- and mode-dependent attenuation, dispersion, and coupling) are identified from first principles and expressed in terms of the statistical properties of the index of refraction of the water column and the sea bottom properties. This theoretical analysis makes it possible to formulate an inverse problem for the estimation of the model parameters from the sound pressure recorded by a vertical hydrophone array and transmitted by distant time-harmonic sources. This inverse problem is solved using data collected during the ALMA 2016 experiment.

In the experimental configuration addressed in this paper, it turns out that radiation effects can be neglected (compared to dissipation in the sediments) and non-Gaussian scintillation effects can be neglected as well. The extraction of the frequency-dependent correlation radii of the recorded sound pressure signals makes it possible to estimate different acoustic and geoacoustic parameters: the sediment sound speed c_s, the standard deviation of the index of refraction in the water column σ, the attenuation parameter in the sediments α, and the vertical correlation radius of the index of refraction in the water column ℓ_v can be robustly estimated, although the Bayesian analysis reveals some correlations between σ, ℓ_v, and α. The sediment density ρ_s and the horizontal correlation radius ℓ_h are difficult to estimate, because they have small effects on the correlation radii of the sound pressure.

ACKNOWLEDGMENTS

We thank Dominique Fattaccioli and Gaultier Real from Direction Générale de l'Armement (DGA) Naval Systems for interesting discussions and for making the ALMA 2016 data available to us. We also thank Julien Bonnel for stimulating discussions.

APPENDIX A: WAVE MODE DECOMPOSITION

Let us introduce the Helmholtz operator

$$\mathcal{H} = \rho_0(z)\partial_z \rho_0(z)^{-1}\partial_z + \omega^2 c_0(z)^{-2}, \tag{A1}$$

where $\rho_0(z) = \rho_w 1_{[0,z_b]}(z) + \rho_s 1_{(z_b,+\infty)}(z)$, with the Dirichlet boundary condition at the top: $\phi(0) = 0$ and continuity conditions at $z = z_b$ and $\phi'(z_b^-)/\rho_w = \phi'(z_b^+)/\rho_s$. The Helmholtz operator $\mathcal{H}$ is self-adjoint with respect to the scalar product defined on $L^2(\mathbb{R}^+, \rho_0^{-1})$ by

$$\begin{aligned}(\phi_1, \phi_2)_{L^2} :&= \int_0^\infty \rho_0^{-1}(z)\,\overline{\phi_1(z)}\,\phi_2(z)dz \\ &= \rho_w^{-1}\int_0^{z_b} \overline{\phi_1(z)}\phi_2(z)dz + \rho_s^{-1} \\ &\quad \times \int_{z_b}^{+\infty} \overline{\phi_1(z)}\phi_2(z)dz.\end{aligned} \tag{A2}$$

The Helmholtz operator has a spectrum of the form (3) where the N modal wavenumbers k_{zj} are positive and $k_s^2 < k_{zN}^2 < \cdots < k_{z1}^2 < k_w^2$.

Discrete spectrum. The jth eigenvector associated with the eigenvalue k_{zj}^2 is

$$\phi_j(z) = \begin{cases} \chi_j \sin(\sigma_j z/z_b) & \text{if } 0 \le z \le z_b, \\ \chi_j \sin(\sigma_j)\exp(-\zeta_j(z-z_b)/z_b) & \text{if } z \ge z_b, \end{cases} \tag{A3}$$

where

$$\sigma_j = z_b\sqrt{k_w^2 - k_{zj}^2}, \quad \zeta_j = z_b\sqrt{k_{zj}^2 - k_s^2}, \tag{A4}$$

$$\chi_j^2 = \frac{2/z_b}{\frac{1}{\rho_w}\left(1 - \frac{\sin(2\sigma_j)}{2\sigma_j}\right) + \frac{1}{\rho_s}\frac{\sin^2(\sigma_j)}{\zeta_j}}. \tag{A5}$$

The σ_j's are the solutions in $\left(0, \sqrt{k_w^2 - k_s^2}z_b\right)$ of

$$\tan(\sigma) = -\frac{\sigma}{\sqrt{z_b^2(k_w^2 - k_s)^2 - \sigma^2}}\frac{\rho_s}{\rho_w}, \tag{A6}$$

and N is the number of solutions.

Continuous spectrum. For $\gamma \in (-\infty, k_s^2)$, the improper eigenvector has the form

$$\phi_\gamma(z) = \begin{cases} \chi_\gamma \sin(\eta_\gamma z/z_b) & \text{if } 0 \le z \le z_b, \\ \chi_\gamma\left[\sin(\eta_\gamma)\cos(\xi_\gamma(z-z_b)/z_b)\right. & \\ \quad \left. + \frac{\rho_s}{\rho_w}\frac{\eta_\gamma}{\xi_\gamma}\cos(\eta_\gamma)\sin(\xi_\gamma(z-z_b)/z_b)\right], & \text{if } z \ge z_b, \end{cases} \tag{A7}$$

where

$$\eta_\gamma = z_b\sqrt{k_w^2-\gamma}, \quad \xi_\gamma = z_b\sqrt{k_s^2-\gamma}, \tag{A8}$$

$$\chi_\gamma^2 = \frac{\xi_\gamma \rho_s z_b}{\pi\left(\xi_\gamma^2\sin^2(\eta_\gamma) + \frac{\rho_s^2}{\rho_w^2}\eta_\gamma^2\cos^2(\eta_\gamma)\right)}. \tag{A9}$$

We remark that ϕ_γ does not belong to $L^2(\mathbb{R}^+,\rho_0^{-1})$, but $(\phi_\gamma,\phi)_{L^2}$ can be defined for any test function $\phi\in L^2(\mathbb{R}^+,\rho_0^{-1})$ as

$$(\phi_\gamma,\phi)_{L^2} = \lim_{M\to+\infty}\int_0^M \phi_\gamma(z)\phi(z)\rho_0(z)^{-1}dz, \tag{A10}$$

where the limit holds on $L^2((-\infty,k_s^2))$.

Completeness. We have for any $\phi\in L^2(\mathbb{R}^+,\rho_0^{-1})$,

$$(\phi,\phi)_{L^2} = \sum_{j=1}^N |(\phi_j,\phi)_{L^2}|^2 + \int_{-\infty}^{k_s^2} |(\phi_\gamma,\phi)_{L^2}|^2 d\gamma. \tag{A11}$$

The map that assigns the coefficients of its spectral decomposition to every element of $\phi\in L^2(\mathbb{R}^+,\rho_0^{-1})$,

$$\phi\mapsto\Big((\phi_j,\phi)_{L^2}, j=1,\dots,N, (\phi_\gamma,\phi)_{L^2}, \gamma\in(-\infty,k_s^2)\Big)$$

is an isometry from $L^2(\mathbb{R}^+,\rho_0^{-1})$ onto $\mathbb{C}^N\times L^2((-\infty,k_s^2))$. This means that any function $\phi\in L^2(\mathbb{R}^+,\rho_0^{-1})$ can be expanded on the set of the eigenfunctions of $\mathcal{H}$.

APPENDIX B: THE EFFECTIVE MARKOVIAN SYSTEM FOR THE COMPLEX MODE AMPLITUDES

We assume that the reduced wavenumbers $(k_{zj})_{j=1}^N$ are distinct. Then, for any $x_\infty>0$, the process $((\hat a_j^\varepsilon(x))_{j=1}^N, (\hat a_\gamma^\varepsilon(x))_{\gamma\in((0,k_s^2))})$ converges in distribution in $\mathcal{C}^0([0,x_\infty],\mathbb{C}^N\times L^2((0,k_s^2)))$, the space of continuous functions from $[0,x_\infty]$ to $\mathbb{C}^N\times L^2((0,k_s^2))$, to the Markov process $((a_j(x))_{j=1}^N, (a_\gamma(x))_{\gamma\in(0,k_s^2)})$ with infinitesimal generator $\mathcal{L}$. Here, $\mathbb{C}^N\times L^2((0,k_s^2))$ is equipped with the weak topology and the infinitesimal generator $\mathcal{L}=\mathcal{L}^1+\mathcal{L}^2+\mathcal{L}^3$ where $\mathcal{L}^j$, $1\le j\le 3$, are the differential operators

$$\begin{aligned}\mathcal{L}^1 =& \frac{1}{2}\sum_{j,l=1}^N \Gamma_{jl}\big(a_j\overline{a_j}\partial_{a_l}\partial_{\overline{a_l}} + a_l\overline{a_l}\partial_{a_j}\partial_{\overline{a_j}} - a_ja_l\partial_{a_j}\partial_{a_l}\\ &-\overline{a_j}\overline{a_l}\partial_{\overline{a_j}}\partial_{\overline{a_l}}\big)\mathbf{1}_{j\neq l} + \frac{1}{2}\sum_{j,l=1}^N \Gamma_{jl}^1\big(a_j\overline{a_l}\partial_{a_j}\partial_{\overline{a_l}} + \overline{a_j}a_l\partial_{\overline{a_j}}\partial_{a_l}\\ &-a_ja_l\partial_{a_j}\partial_{a_l} - \overline{a_j}\overline{a_l}\partial_{\overline{a_j}}\partial_{\overline{a_l}}\big) + \frac{1}{2}\sum_{j=1}^N\Big(\Gamma_{jj}-\Gamma_{jj}^1\Big)\\ &\times\big(a_j\partial_{a_j}+\overline{a_j}\partial_{\overline{a_j}}\big) + \frac{i}{2}\sum_{j=1}^N\Gamma_{jj}^s\big(a_j\partial_{a_j}-\overline{a_j}\partial_{\overline{a_j}}\big),\end{aligned} \tag{B1}$$

$$\mathcal{L}^2 = -\frac{1}{2}\sum_{j=1}^N(\Lambda_j+i\Lambda_j^s)a_j\partial_{a_j} + (\Lambda_j-i\Lambda_j^s)\overline{a_j}\partial_{\overline{a_j}}, \tag{B2}$$

$$\mathcal{L}^3 = i\sum_{j=1}^N \kappa_j\big(a_j\partial_{a_j}-\overline{a_j}\partial_{\overline{a_j}}\big). \tag{B3}$$

In these definitions, we use the classical complex derivative: if $\zeta=\zeta_r+i\zeta_i$, then $\partial_\zeta=(1/2)(\partial_{\zeta_r}-i\partial_{\zeta_i})$ and $\partial_{\bar\zeta}=(1/2)(\partial_{\zeta_r}+i\partial_{\zeta_i})$, and the coefficients of the operators (B1)–(B3) are defined for $j,l=1,\dots,N$, as follows.

- For all $j\neq l$, Γ_{jl} is defined by Eq. (30) and

$$\Gamma_{jl}^s = \frac{\omega^4}{2k_{zj}k_{zl}}\int_0^\infty \mathcal{R}_{jl}^w(x)\sin\big[(k_{zl}-k_{zj})x\big]dx,$$

  with $\mathcal{R}_{jl}^w(x)$ defined by Eq. (32).
- For all j,l,

$$\Gamma_{jl}^1 = \frac{\omega^4}{2k_{zj}k_{zl}}\int_0^\infty \mathbb{E}\big[C_{jj}^w(0)C_{ll}^w(x)\big]dx.$$

- For all j, Λ_j is defined by Eq. (31) and

$$\begin{aligned}\Gamma_{jj} &= -\sum_{l=1,l\neq j}^N\Gamma_{jl}, \quad \Gamma_{jj}^s = -\sum_{l=1,l\neq j}^N\Gamma_{jl}^s,\\ \Lambda_j^s &= \int_0^{k_s^2}\frac{\omega^4}{2\sqrt{\gamma}k_{zj}}\int_0^\infty \mathcal{R}_{j\gamma}^w(x)\sin\big[\big(\sqrt{\gamma}-k_{zj}\big)x\big]dxd\gamma,\\ \kappa_j &= \int_{-\infty}^0\frac{\omega^4}{2\sqrt{|\gamma|}k_{zj}}\int_0^\infty \mathcal{R}_{j\gamma}^w(x)\cos(k_{zj}x)e^{-\sqrt{|\gamma|}x}dxd\gamma.\end{aligned}$$

Remarks

(1) The convergence result holds in the weak topology (this follows from the proof that is based on the perturbed test function method[22]). This means that we can only compute quantities of the form $\mathbb{E}[F(a_1,\dots,a_N,\int_0^{k_s^2}\alpha_\gamma a_\gamma d\gamma)]$ for any test functions $\alpha\in L^2((0,k_s^2))$ and $F:\mathbb{R}^{N+1}\to\mathbb{R}$, which are the limits of $\mathbb{E}[F(\hat a_1^\varepsilon,\dots,\hat a_N^\varepsilon,\int_0^{k_s^2}\alpha_\gamma\hat a_\gamma^\varepsilon d\gamma)]$ as $\varepsilon\to 0$.

(2) The generator $\mathcal{L}$ does not involve ∂_{a_γ}. This shows that $(\hat a_j^\varepsilon(x))_{j=1}^N$ converges in distribution in $\mathcal{C}^0([0,x_\infty],\mathbb{C}^N)$ to the Markov process $(a_j(x))_{j=1}^N$ with generator $\mathcal{L}$. The weak and strong topologies are the same in $\mathbb{C}^N$, so we can compute any moment of the form $\mathbb{E}[F(a_1,\dots,a_N)]$, which are the limits of $\mathbb{E}[F(\hat a_1^\varepsilon,\dots,\hat a_N^\varepsilon)]$.

(3) $\mathcal{L}_1$ is the contribution of the coupling between guided modes, which gives rise to power exchange between the guided modes; $\mathcal{L}_2$ is the contribution of the coupling between guided and radiating modes, which gives rise to power leakage from the guided modes to the radiating ones (effective diffusion) and addition of frequency-dependent phases on the guided modes (effective dispersion); $\mathcal{L}_2$ also contains the effective mode-dependent term due to dissipation in the sediments; $\mathcal{L}_3$ is the contribution of the coupling between guided and evanescent modes, which gives rise to additional phase terms on the guided modes (effective dispersion[23]).

(4) If the generator $\mathcal{L}$ is applied to a test function that depends only on the mode powers $(P_j=|a_j|^2)_{j=1}^N$, then

the result is a function that depends only on $(P_j)_{j=1}^N$. This shows that[22] the mode powers $(P_j(x))_{j=1}^N$ define a Markov process, with the generator given by Eq. (29).

(5) The radiation mode amplitudes remain constant on $L^2((0,k_s^2))$, equipped with the weak topology, as $\varepsilon \to 0$. This does not describe, however, the power $\int_0^{k_s^2} |\hat{a}_\gamma^\varepsilon|^2 d\gamma$ transported by the radiation modes, because the convergence does not hold in the strong topology of $L^2((0,k_s^2))$, so we do not have $\int_0^{k_s^2} |\hat{a}_\gamma^\varepsilon|^2 d\gamma \to \int_0^{k_s^2} |a_\gamma|^2 d\gamma$ as $\varepsilon \to 0$.

[1]J. Garnier and G. Papanicolaou, "Pulse propagation and time reversal in random waveguides," SIAM J. Appl. Math. **67**, 1718–1739 (2007).
[2]C. Gomez, "Wave propagation in shallow-water acoustic random waveguides," Commun. Math. Sci. **9**, 81–125 (2011).
[3]W. Kohler and G. Papanicolaou, "Wave propagation in randomly inhomogeneous ocean," in *Lecture Notes in Physics, Wave Propagation and Underwater Acoustics*, edited by J. B. Keller and J. S. Papadakis (Springer Verlag, Berlin, 1977), Vol. 70.
[4]L. Borcea, J. Garnier, and C. Tsogka, "A quantitative study of source imaging in random waveguides," Commun. Math. Sci. **13**, 749–776 (2015).
[5]M. J. Beran and S. Frankenthal, "Volume scattering in a shallow channel," J. Acoust. Soc. Am. **91**, 3203–3211 (1992).
[6]J. A. Colosi and A. Morozov, "Statistics of normal mode amplitudes in an ocean with random sound speed perturbations: Cross mode coherence and mean intensity," J. Acoust. Soc. Am. **126**, 1026–1035 (2009).
[7]J. A. Colosi, T. F. Duda, and A. K. Morozov, "Statistics of low-frequency normal-mode amplitudes in an ocean with random sound-speed perturbations: Shallow-water environments," J. Acoust. Soc. Am. **131**, 1749–1761 (2012).
[8]D. Creamer, "Scintillating shallow water waveguides," J. Acoust. Soc. Am. **99**, 2825–2838 (1996).
[9]L. B. Dozier and F. D. Tappert, "Statistics of normal-mode amplitudes in a random ocean. I. Theory," J. Acoust. Soc. Am. **63**, 353–365 (1978).
[10]L. B. Dozier and F. D. Tappert, "Statistics of normal-mode amplitudes in a random ocean. II. Computations," J. Acoust. Soc. Am. **64**, 533–547 (1978).
[11]A. B. Baggeroer, W. A. Kuperman, and P. N. Mikhalevsky, "An overview of matched field methods in ocean acoustics," IEEE J. Ocean. Eng. **18**, 401–424 (1993).
[12]M. Siderius, P. L. Nielsen, J. Sellschopp, M. Snellen, and D. Simons, "Experimental study of geo-acoustic inversion uncertainty due to ocean sound-speed fluctuations," J. Acoust. Soc. Am. **110**, 769–781 (2001).
[13]L. B. Dozier, "A coupled mode model for spatial coherence of bottom-interacting energy," in *Proceedings of the Stochastic Modeling Workshop*, edited by C. W. Spofford and J. M. Haynes, ARL-University of Texas, Austin, TX, 1983.
[14]F. B. Jensen, W. A. Kuperman, M. B. Porter, and H. Schmidt, *Computational Ocean Acoustics* (Springer, New York, 1993), Chap. 5.
[15]S. M. Flatté, R. Dashen, W. H. Munk, K. M. Watson, and F. Zachariasen, *Sound Transmission Through a Fluctuating Ocean* (Cambridge University Press, Cambridge, 1979).
[16]J. Zhou, "Normal mode measurements and remote sensing of sea-bottom sound velocity and attenuation in shallow water," J. Acoust. Soc. Am. **78**, 1003–1009 (1985).
[17]J. X. Zhou, X. Z. Zhang, and D. P. Knobles, "Low-frequency geoacoustic model for the effective properties of sandy seabottoms," J. Acoust. Soc. Am. **125**, 2847–2866 (2009).
[18]J. X. Zhou, X. Z. Zhang, P. H. Rogers, J. A. Simmen, P. H. Dahl, G. Jin, and Z. Peng, "Reverberation vertical coherence and sea-bottom geoacoustic inversion in shallow water," IEEE J. Ocean. Eng. **29**, 988–999 (2004).
[19]L. Wan, M. Badiey, and D. P. Knobles, "Geoacoustic inversion using low frequency broadband acoustic measurements from L-shaped arrays in the Shallow Water 2006 Experiment," J. Acoust. Soc. Am. **140**, 2358–2373 (2016).
[20]D. Fattaccioli, "ALMA: A new experimental acoustic system to explore coastal and shallow waters," UACE 2015 Proceedings, Chania, Greece.
[21]C. Wilcox, "Spectral analysis of the Pekeris operator in the theory of acoustic wave propagation in shallow water," Arch. Rational Mech. Anal. **60**, 259–300 (1976).
[22]J.-P. Fouque, J. Garnier, G. Papanicolaou, and K. Sølna, *Wave Propagation and Time Reversal in Randomly Layered Media* (Springer, New York, 2007).
[23]J. Garnier, "The role of evanescent modes in randomly perturbed single-mode waveguides," Discr. Cont. Dyn. Syst. B **8**, 455–472 (2007).
[24]C. Garrett and W. H. Munk, "Internal waves in the ocean," Annu. Rev. Fluid Mech. **11**, 339–369 (1979).
[25]C. R. MacCluer, "The many proofs and applications of Perron's theorem," SIAM Rev. **42**, 487–498 (2000).
[26]D. Fattaccioli and G. Real, "The DGA 'ALMA' Project: An overview of the recent improvements of the system capabilities and of the at-sea campaign ALMA-2016," UACE 2017 Proceedings (Skiathos, Greece), available at www.uaconferences.org/docs/2017_papers/649_UACE2017.pdf (Last viewed July 9, 2019).
[27]R. H. Byrd, P. Lu, J. Nocedal, and C. Zhu, "A limited memory algorithm for bound constrained optimization," SIAM J. Sci. Comput. **16**, 1190–1208 (1995).
[28]M. D. Richardson and K. B. Briggs, "Empirical predictions of seafloor properties based on remotely measured sediment impedance," AIP Conf. Proc. **728**, 12–21 (2004).
[29]A. Saltelli, M. Ratto, T. Andres, F. Campolongo, J. Cariboni, D. Gatelli, M. Saisana, and S. Tarantola, *Global Sensitivity Analysis. The Primer* (Wiley, Hoboken, 2008).
[30]Service Hydrographique et Océanographique de la Marine, available at data.shom.fr (Last viewed July 9, 2019).